Available online at www.sciencedirect.com
ScienceDirect
Trans. Nonferrous Met. Soc. China 24(2014) 3356−3365
Transactions of Nonferrous Metals Society of China
www.tnmsc.cn

Crystallization behaviors of bayerite from sodium chromate alkali solutions

Guang-ye WEI[1,2], Jing-kui QU[1], Yu-dong ZHENG[2], Tao QI[1], Qiang GUO[1], Bing-bing HAN[1], Hong-xin ZHAO[1]

1. National Engineering Laboratory for Hydrometallurgical Cleaner Production Technology, Institute of Process Engineering, Chinese Academy of Sciences, Beijing 100190, China;
2. School of Materials Science and Engineering, University of Science and Technology, Beijing 10083, China

Received 10 October 2013; accepted 25 February 2014

Abstract: In order to clean production of chromium compounds, it is a critical process to remove aluminates and utilize aluminum compounds from artificial chromate alkali solutions. The effects of Na_2CrO_4 on the neutralization curve, $Al(OH)_3$ precipitation efficiency and induction period of bayerite were investigated. The results indicate that the neutralization curve of the artificial chromate alkali solutions shows three distinct regions and its induction period is longer than that of pure sodium aluminate solutions at the same aluminum concentration. And the decreased temperature and volume fraction of CO_2 enhance the particle size of bayerite β-$Al(OH)_3$. Bayerite composed of agglomerates of rods and cone frustums was obtained from alkali metal chromate solutions with 28.5% CO_2 (volume fraction) at temperatures ranging from 50 °C to 70 °C. Coarse bayerite with particle size (d_{50}) from 24.2 μm to 29.3 μm extremely has few impurities, which is suitable for comprehensive utilization.
Key words: chromate alkali solutions; bayerite; carbonization; crystallization; precipitation efficiency

1 Introduction

Chromium compounds have attracted considerable interest because of their wide application in pigments [1], coating materials for thermal protection [2], catalysts [3], glass production [4] and lithium ion batteries [5]. The traditional process of producing chromium compounds from chromium ores generally involves a high-temperature roasting reaction. The roasted product is usually leached with water or solutions containing an alkali metal carbonate or hydroxide. The leaching liquor contains chromates and alkali metal aluminates as well as other foreign substances.

Several improvements have been made to remove Al from chromium leaching liquors by addition of acids, soluble silica compounds [6] and CaO [7]. Precipitates of aluminum compound are gelatinous, and their filtration is highly time-consuming. It was reported a process for preparing pure alkali metal solutions by addition of acids prior to the separation of insoluble components [8]. The sludge in this work exhibits surprisingly favorable filtration properties in comparison with gelatinous aluminum hydroxide $Al(OH)_3$. The process of Al removal used by Allied Chemical Corporation involves the removal of dissolved aluminates by seed precipitation [9]. However, the overall residence time in the series of vessels ordinarily ranges from approximately 9 h to 12 h.

SMELLIE and BRANASTATTER [10] provided a process for removing aluminates by acidification using CO_2 at temperatures ranging from 5 °C to 10 °C and elevated pressure. A carbonization process has also been used to remove Al after the separation of sodium aluminum silicate under atmospheric conditions [11]. Given the low cost and wide availability of CO_2, it has further been used to recover Al from red mud or etching waste streams of the aluminum industry through carbonization. The carbonization process can be maintained at high supersaturation levels because of the continuous introduction of CO_2 gas into alkaline solutions [12,13]. Thus, the precipitation rate of carbonization is significantly faster than that of seed precipitation [14]. The mechanism of carbonization in chromate alkali solutions remains unclear despite a previous patented research [15].

Foundation item: Project (51125018) supported by the National Science Found for Distinguished Young Scholars of China; Project (2011BAC06B07) supported by the National Key Technologies R&D Program of China; Project (2011AA060704) supported by the National Hi-tech Research and Development Program of China; Projects (51204153, 21106167) supported by the National Natural Science Foundation of China; Projects (2012M510552, 2013T60175) supported by Financial Grant from the China Postdoctoral Science Foundation
Corresponding author: Tao QI; Tel: +86-10-62631710; E-mail: tqgreen@home.ipe.ac.cn
DOI: 10.1016/S1003-6326(14)63477-4

In the investigation of $Al(OH)_3$ precipitates, a large amount of chromate in pure sodium aluminate solutions was considered as an impurity. The effects of other impurities on the solubility and crystallization behavior of gibbsite were investigated. At the same alkali metal solution concentration, the equilibrium Al(III) solubility of a Bayer liquor is higher than that of pure sodium aluminate solutions because of the presence of impurities (carbonates and sulfates) [16]. Therefore, a large amount of chromate may have significant effects on the equilibrium solubility of $Al(OH)_3$ and the driving force in nucleation and growth processes. Furthermore, large amounts of inorganic impurities may have inhibitory effects on the morphology or agglomeration of $Al(OH)_3$ particles during the crystallization step [17,18]. Changing the external conditions, such as increasing the driving force and/or sodium caustic concentrations, has no significant effect on the morphology of the particles. However, changing the alkali ions in the sodium caustic solution largely affects the crystal morphology of $Al(OH)_3$. The highest impurity content yields the lowest crystal growth rate at 60 °C [19]. Thus, crystallization behavior of $Al(OH)_3$ in chromate alkali solutions needs more researches.

In this work, the effects of sodium chromate (Na_2CrO_4), temperature and volume fraction of CO_2 on the induction period, precipitation efficiency and crystallite size of bayerite from chromate alkali solutions were investigated. The main objective of this study is to investigate the crystallization of bayerite in the presence of a large amount of chromate under low volume fraction of CO_2 and at ambient atmosphere. Optimum conditions for the precipitation of low-impurity bayerite from chromate alkali solutions were also determined.

2 Experimental

2.1 Chemicals

Analytical-reagent grade pure $Al(OH)_3$, sodium hydroxide (NaOH), and Na_2CrO_4 were purchased from Guangdong Xilong Chemical Co., Ltd., China. CO_2 (99.99%) and nitrogen (99.99%) gases were obtained from Sinopharm Chemical Reagent Beijing Co., Ltd., China. Sodium aluminate solutions were prepared by reacting 15.0 g $Al(OH)_3$ with 33.0 g NaOH in water. Afterward, 350 g Na_2CrO_4 and deionized water were added to the mixture to obtain 1 L $NaOH{-}Na_2AlO_2{-}Na_2CrO_4{-}H_2O$ solution (chromate alkali solution).

2.2 Procedures

The experiments were performed in a three-necked flask with a glass lid featuring the necessary outlets for a mechanical stirrer, a Pt thermocouple, a double-surface condenser and a pH electrode. The flask was heated by an electric oil bath, and the temperature was controlled by a proportional-integral-derivative controller. The experimental controller was set up according to Ref. [14]. The neutralization curve was obtained using a pH meter (Mettler-Toledo SevenMulti S40, Switzerland).

The chromate alkali solution (480 mL) was stirred in the flask at an agitation rate of 120 r/min while heating until the preset temperature. At this time (t=0), the present experiments on various mixtures of N_2 and CO_2 gases were conducted at constant temperature. The flow rate of the mixture was measured and controlled by a rotary flowmeter, and the total flow rate of the N_2 and CO_2 mixtures was 0.6 L/min.

After the reaction, the slurry in the flask was filtered using a Buchner funnel. The residue was washed with deionized water at 90 °C for 30 min. After complete washing, the residue ($Al(OH)_3$ series) was air-dried at 105 °C in an electric blast drying oven.

The residual concentration of aluminum in the filtrate was analyzed by inductively coupled plasma optical emission spectrometer (ICP-OES, Optimal 5300 DV, Perkin Elmer Instruments, USA). The precipitation efficiency of the $Al(OH)_3$ sample was calculated as follows:

$$X = (1 - C_r V_r / C_i V_i) \times 100\% \quad (1)$$

where X is the precipitation efficiency; C_i and C_r are the initial and residual aluminum concentrations, respectively; V_i and V_r are the initial and residual solution volumes, respectively.

The chromium and sodium contents of $Al(OH)_3$ were further determined by ICP-OES. X-ray analysis was performed on a TTRAX3 theta goniometer (powder X-ray diffractometer) using Cu K_α radiation in step mode between 10° and 90°. The step size was 0.01°, and the step time was 0.3 s. The d spacings were calculated using X'pert HighScore software. The surface morphology and particle size distribution of the samples were investigated with a scanning electron microscope (JSM 6700F, Japan) and a mastersizer (MS 2000, England), respectively. The FTIR spectra of bayerite were obtained by direct transmittance using the KBr pellet technique. Pellets of about 1 mg of cellulosic samples were prepared by mixing with 100 mg of spectroscopic-grade KBr. The FTIR spectra were recorded using a Nicolet 520P spectrometer equipped with a detector at 4 cm^{-1} resolution and 64 scans per sample. Background spectra were collected using pure KBr.

3 Results and discussion

3.1 Neutralization curve

In mild-to-strong alkaline solutions, Al^{3+}, $Al(OH)_2^+$, $Al(OH)^{2+}$, $Al(OH)_3^0$ and $Al(OH)_4^-$ are the major complex

ions. Given that $Al(OH)_4^-$ is the only species present in the chromate alkali solution under the applied pH value of 12.5 [20], $Al(OH)_4^-$ in the chromate alkali solution destabilizes and forms the $Al(OH)_3$ precipitate as a result of CO_2 neutralization. The neutralization curve was obtained to describe the pH changes in the solution. As shown in Fig. 1, three regions are observed in the neutralization curve during the carbonization process [21,22].

$$2OH^-(aq)+CO_2(g) \Leftrightarrow CO_3^{2-}(aq)+H_2O(l) \quad (2)$$

$$Al(OH)_4^-(aq) \Leftrightarrow Al(OH)_3(s)+OH^-(aq) \quad (3)$$

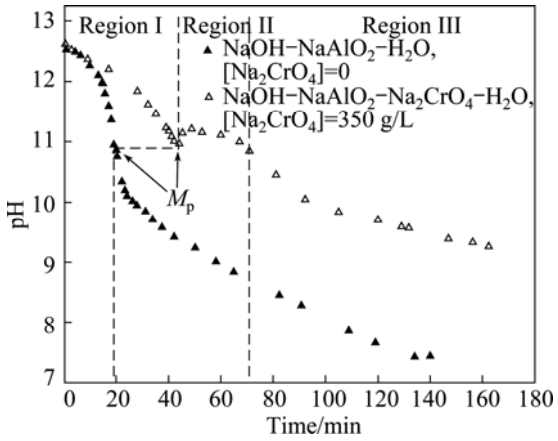

Fig. 1 Neutralization curve obtained at 50 °C ([NaOH] is 33.35 g/L, $[Al_2O_3]$ is 10 g/L, $[Na_2CrO_4]$ is 0 or 350 g/L)

In region I, the pH sharply decreases with time in two curves. This result indicates a spontaneous reaction between the free hydroxide ions and added protons generated from the water-soluble reaction of CO_2 (Eq. (2)). Free hydroxide ions were consumed as more CO_2 was applied in the process. The process exhibited regular curves similar to those observed during acid neutralization and neutralization of sodium bicarbonate in supersaturated sodium aluminate solutions [21,22].

At the onset of region II, the precipitation point (M_p) obtained from the pure sodium aluminate solution was approximated from the M_p of the chromate alkali solution. However, the pH continued to decrease after the M_p because of the low aluminate concentration and high volume fraction of CO_2 in the pure aluminate solution.

Aluminates in the presence of sodium chromate during the carbonization process were described in this section. Before the precipitation point was achieved, fine $Al(OH)_3$ particles readily redissolved in the solution. After the M_p, $Al(OH)_3$ precipitation suddenly occurred (Eq. (3)) and was accompanied by a significant change in the clarity of the solution from transparent to opaque. Afterward, the pH slightly increased. This indicates that the rate of carbonization is lower than that of hydroxide ion liberation according to the chemical reaction in Eq. (3). In addition, the pH remained nearly constant, which indicates equilibrium between the rate of carbonization and rate of hydroxide ion liberation and the high buffering capacity of the chromate alkali solution.

As previously reported, a high buffering capacity usually occurred in supersaturated sodium aluminate solutions with low neutralization rates [21,22]. The alkali metal chromate solution shows nearly the same buffering capacity as supersaturated sodium aluminate solutions. This suggests the hydration of a significant amount of sodium in the solution, which hinders the decomposition of sodium aluminate solutions and results in a longer precipitation time. Moreover, the pH remains constant because of the slow liberation of water from hydrated sodium ions.

In region III, the pH continued to decrease, indicating that the rate of carbonization is higher than that of hydroxide ion liberation. The curve shows a decrease in $Al(OH)_4^-$ concentration followed by continuous bubbling of the CO_2 volume fraction. Therefore, a significantly large $Al(OH)_3$ solid phase continued to precipitate until all of the $Al(OH)_4^-$ ions were completely reacted.

3.2 Precipitation efficiency of $Al(OH)_3$

In the presence of sodium chromate, the precipitation efficiency exceeded 50% (mass fraction) within 63 min and was approximately 89.9% after 108 min of carbonation reaction (Fig. 2). In the absence of sodium chromate, the precipitation efficiency exceeded 70% within 35 min and the precipitation was nearly complete within 60 min.

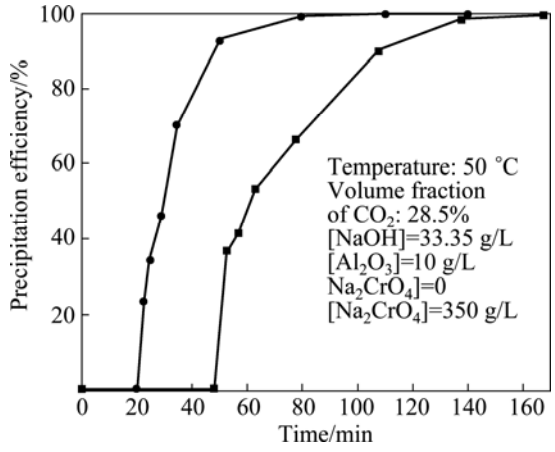

Fig. 2 Effect of sodium chromate on precipitation efficiency of $Al(OH)_3$

$Al(OH)_3$ was precipitated in the pure sodium aluminate solutions within 20 min. By contrast, precipitation in the chromate alkali solution required

48 min. This phenomena was explained as induction period, which was defined as the time required for the pH of the chromate alkali solution to reach the M_p (Fig. 1) in these experiments [23]. In the induction period, the formation of $Al(OH)_3$ nuclei in the solution involved ion pairs of polycondensation reactions of $Al(OH)_4^-$. The induction period was longer in alkali chromate solution than in the unseeded pure sodium aluminate solutions during the carbonation process. The high ionic strength of sodium ions may have hindered the polycondensation reactions in the chromate alkali solution, thus resulting in difficulty in $Al(OH)_3$ precipitation. These results were confirmed by the change of pH in solution.

3.3 Induction period

The results show that increased temperature and CO_2 volume fraction significantly enhance the precipitation of $Al(OH)_3$ (Fig. 3). Nucleation of $Al(OH)_3$ crystals in supersaturated aluminates solutions is a controlled chemical reaction [24]. The induction period was reduced at 30−70 °C for 76−38 min, and the primary product is $Al(OH)_3$. The polycondensation reaction rate of $Al(OH)_4^-$ ions increased and the viscosity of the

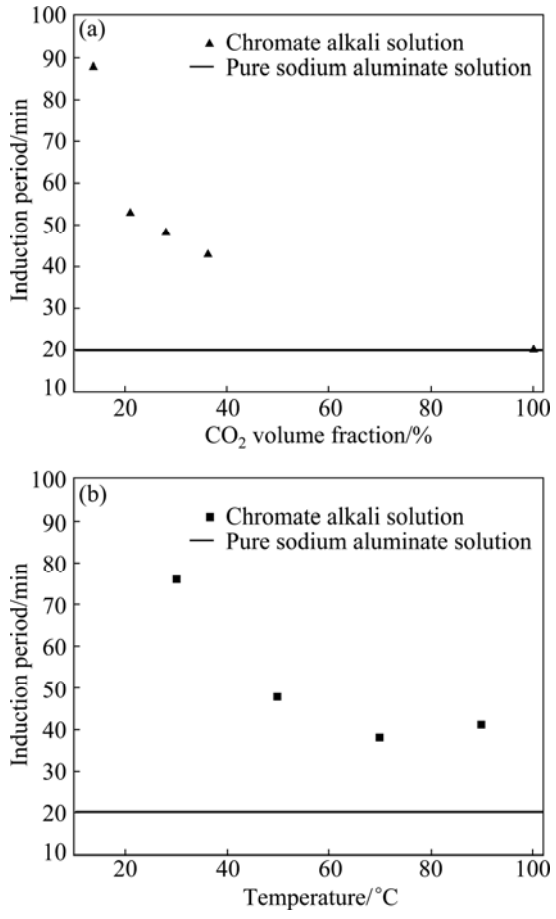

Fig. 3 Induction period as function of temperature and CO_2 volume fraction ([NaOH] is 33.35 g/L, [Al_2O_3] is 10 g/L, [Na_2CrO_4] is 350 g/L)

chromate alkali solution decreased with increasing temperature, thereby resulting in the rapid $Al(OH)_3$ crystallization. The precipitation of $NaAl(OH)_2CO_3$ was more favorable at high temperatures. The reaction is given as follows [25]:

$$Na^+(aq)+Al(OH)^-(aq)+CO_2(g) \Leftrightarrow NaAl(OH)_2CO_3(s)+H_2O(l) \quad (4)$$

As a result, the fine $NaAl(OH)_2CO_3$ particles redissolved and formed stable $Al(OH)_4^-$ ions in the solution. Therefore, the induction period slightly lengthened at 90 °C.

The above reaction indicates that the polycondensation reaction of $Al(OH)_4^-$ can readily occur at high CO_2 volume fractions [15]. Given the low initial sodium hydroxide and low sodium aluminate concentration in the chromate alkali solution, the polycondensation reaction of $Al(OH)_4^-$ ions accelerated, particularly at high CO_2 volume fractions. The induction period was reduced from 88 min to 43 min. At volume fraction of 100% CO_2, the induction period in the chromate solution was shorter than 20 min and identical to that of the pure sodium aluminate solutions.

The induction period depends on the temperature as well as the volume fraction of CO_2. Solution properties, including relative supersaturation, alkali metal species content and concentration, also strongly affect the induction period [23,26]. The induction period was 4 h longer in $NaAl(OH)_4$ than in $KAl(OH)_4$. Sodium ions provided greater stability for the formation and densification of Al(III)-containing clusters. Under similar crystallization conditions, the rate of $Al(OH)_3$ crystallite formation was higher in sodium than in potassium liquors.

In these experiments, the presence of chromate in the solution was the only difference among solutions. For some yet unknown reason, the induction period of the alkali metal solution varied with that of the pure sodium aluminate solution. For homogeneous nucleation, the variation in $\ln\tau$ was linear with respect to $\ln\sigma$ (where σ was the relative supersaturation). Chromate may change the equilibrium solubility of $Al(OH)_3$ and the relative supersaturation of the solution.

According to the research by ADDAI-MENSAH and RALSTON [27], non-DLVO forces or repulsive steric forces are present under synthetic Bayer conditions [27]. At a given condition, hydrodynamic repulsion is lower in the chromate alkali solution compared with in the pure sodium aluminate solution. This is due to its higher solution viscosity of chromate alkali solution. After aging, steric repulsion gradually diminishes, followed by an increase in adhesion. This phenomenon indicates the occurrence of weaker sodium ion-pair interactions between the $Al(OH)_4^-$ and OH^- species in

the chromate alkali solution. During the gradual transformation of $Al(OH)_4^-$ to $Al(OH)_3$, interfacial layer structuring is apparently responsible for at least part of the crystal growth, secondary nucleation and agglomeration mechanisms. At low-particle approach velocities, longer induction periods and lower $Al(OH)_3$ agglomeration rates may be predicted for the chromate alkali solution compared with the pure sodium aluminate solution.

3.4 Characterization of bayerite

3.4.1 XRD analysis and particle size distribution

The XRD pattern of $Al(OH)_3$ crystallization as a function of temperature is shown in Fig. 4(a). Bayerite ($Al(OH)_3$, JCPDS Card No. 12−0457) can be readily obtained from chromate alkali solutions at temperatures below 70 °C. However, dawsonite ($NaAl(OH)_2CO_3$, JCPDS Card No. 19−1175) may be another stable substance that can be produced with CO_2 injection at 90 °C. An improved set of thermodynamic data shows that dawsonite is relatively stable with respect to bayerite at high temperatures. Furthermore, dawsonite formation can occur in moderately basic solutions with higher total carbonate concentrations or the injection of CO_2 which can be described as follows: [25]

$$Na^+(aq) + Al(OH)_3(s) + CO_2(g) + OH^-(aq) \Leftrightarrow NaAl(OH)_2CO_3(s) + H_2O(l) \quad (5)$$

$$Na^+(aq) + Al(OH)_3(s) + HCO_3^-(aq) \Leftrightarrow NaAl(OH)_2CO_3(s) + H_2O(l) \quad (6)$$

Figure 5(a) shows that bayerite is the dominant phase, and little or no dawsonite precipitation occurs at relatively low CO_2 conditions during the carbonation process [12]. There is a small amount of dawsonite forming at a higher CO_2 volume fraction of 36.3%. This is due to dawsonite formation which is the most favorable when CO_2 sequestration reactions are performed under sequestration cycles with CO_2 amount exceeding 50% [28]. In addition, the high solubility of $NaAl(OH)_2CO_3$ at low volume fraction of CO_2 and low temperatures is unlikely to provide the geochemical conditions required for $NaAl(OH)_2CO_3$ formation. These results imply that the experimental conditions, such as temperature and CO_2 volume fraction, must be precisely controlled to produce bayerite. Hence, $Al(OH)_3$

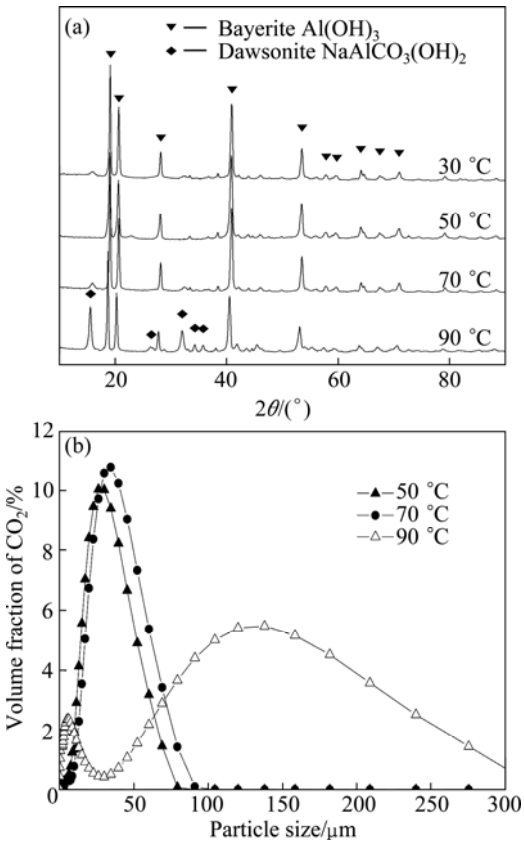

Fig. 4 XRD pattern (a) and particle size distribution (b) as function of temperature on crystallization of bayerite from chromate alkali solutions (Time is 180 min, CO_2 volume fraction is 28.5%, [NaOH] is 33.35 g/L, [Al_2O_3] is 10 g/L, [Na_2CrO_4] is 350 g/L)

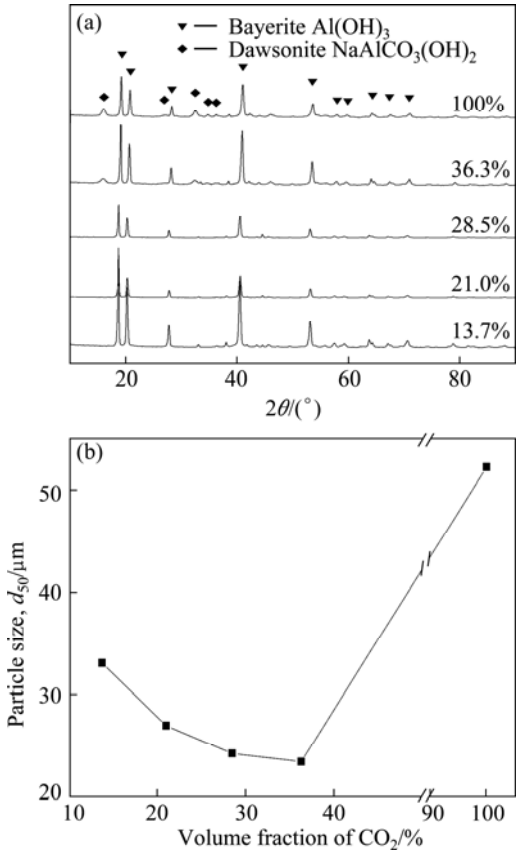

Fig. 5 XRD pattern (a) and particle size distribution (b) as function of CO_2 volume fraction on crystallization of bayerite from chromate alkali solutions (Temperature is 50 °C, time is 180 min, [NaOH] is 33.35 g/L, [Al_2O_3] is 10 g/L, [Na_2CrO_4] is 350 g/L)

precipitation can be obtained from the chromate alkali solution with low initial aluminum concentrations.

Figure 5(b) shows the particle size distribution of the bayerite precipitated from chromate alkali solutions at various temperatures. A bayerite colloidal suspension was obtained at 30 °C. The particle size of bayerite increased with increasing temperature. A narrow size distribution was obtained at the temperature from 50 °C to 70 °C. The particle sizes (d_{50}) of bayerite were 24.2 and 29.3 μm at 50 and 70 °C, respectively. A mixture of fine and coarse particles was obtained at 90 °C, indicating that two different phases coexist in the samples. Figure 5(b) shows that the d_{50} of bayerite decreased from 33.0 to 23.4 μm as the CO_2 volume fraction increased from 13.7% to 36.3%. The d_{50} significantly decreased to 52.2 μm under CO_2 volume fraction of 100%. These results show that the dawsonite phase generally occurs at high temperatures and high CO_2 volume fractions during the carbonation process. Coarse particles were observed as a result of needle-like and wire-like dawsonite twining around the bayerite crystals.

3.4.2 Crystallization and morphology

$Al(OH)_3$ precipitation from the sodium chromate solution is expected to show variations from pure sodium aluminate solutions at the same concentrations. An induction period of 48 min to 38 min was obtained in these experiments. This indicates that the solubility of $Al(OH)_3$ may be improved by the addition of inorganic salt impurities [16]. In the current work, a large amount of sodium chromate affected the equilibrium solubility and supersaturation of the solution.

The deposition rates of aluminates were low in the chromate alkali solution with low supersaturation, resulting in the growth of coarse particles in the solution. This indicates that a suitable induction period leads to well-crystallized bayerite particles. The major phase is bayerite, and its diffraction peaks are strong, either in the early or later stages (Figs. 6(a) and (b)). Meanwhile, the presence of gibbsite as an impurity is usual in bayerite synthesis involving precipitation from sodium aluminate solutions due to thermodynamically stable gibbsite [29]. However, the formation of bayerite in these samples is favorable because of the solution pH as well as the experimental conditions.

As shown in Fig. 7(a), bayerite particles with shapes ranging from agglomerates of rods to cone frustums were obtained from the chromate alkali solutions. The frustums generally existed as twinning crystals that were connected through their top surfaces. Thin plate structures were generally observed in the middle of the twinning crystals, and a large number of frustums were connected with one another by their edges. The rods consisted of several thin plates. The crystals obtained from the chromate alkali solution tended to form twinning crystals of frustums rather than thin plates for 5 min after the M_p (Fig. 1).

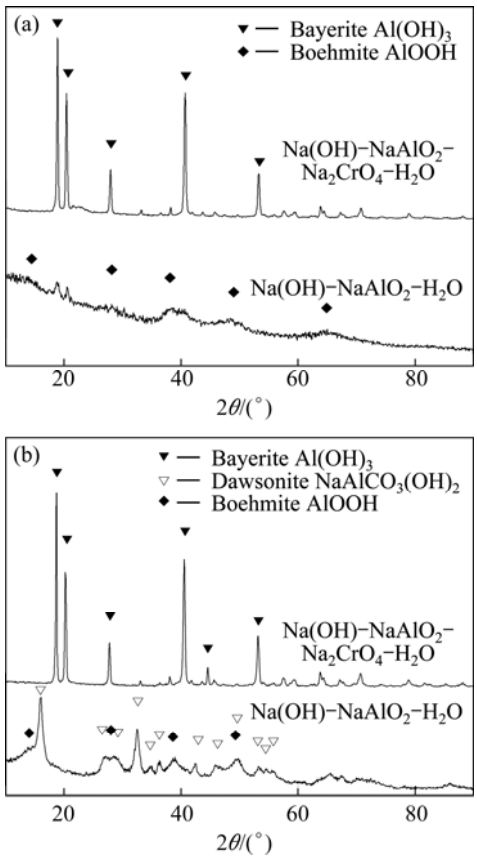

Fig. 6 XRD patterns of samples synthesized at 5 min (a) and 120 min (b) after precipitate point from pure sodium aluminate solution and chromate alkali solution (Temperature is 50 °C, CO_2 volume fraction is 28.5%, [NaOH] is 33.35 g/L, [Al_2O_3] is 10 g/L)

The morphology of the bayerite obtained in this experiment was different from that precipitated from supersaturated sodium aluminate solutions. In the previous work, agglomerates of cones were also observed, and only bunches of cones with a common nucleus were found at the highest pH value (pH=10.4) [30]. Therefore, the irregularity of the basal face edge of the crystals may be expected. Some of the crystals were slightly rounded, whereas others presented a zigzag pattern. Irregular basal faces were also observed in the microrod basal faces of the bayerite synthesized from a low-concentration sodium aluminate solution [29,30]. These may be attributed to variations in crystallization conditions (pH, sodium caustic concentration and time) rather than the presence of large amounts of inorganic impurities [17].

Crystal growth was attributed to the continuous bubbling of CO_2 in the solution with increasing time. Figure 7(b) shows that the size of the frustum twinning

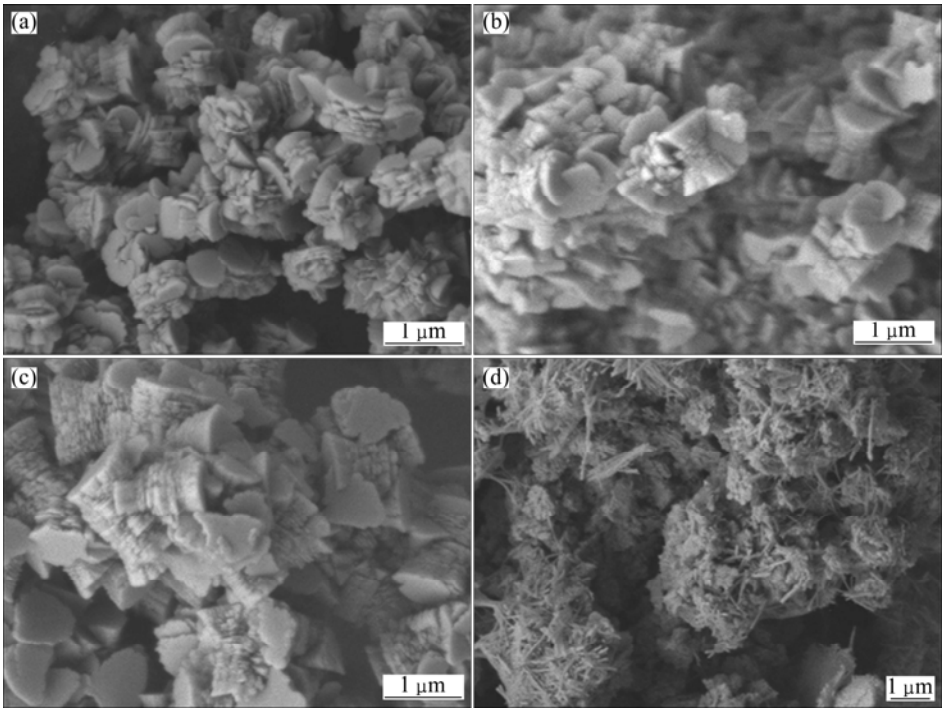

Fig. 7 SEM images of bayerite particles synthesized at 5 min (a), 15 min (b), 30 min (c) and 90 min (d) after precipitation point from chromate alkali solution (Temperature is 50 °C, [NaOH] is 33.35 g/L, CO_2 volume fraction is 28.5%, [Al_2O_3] is 10 g/L, [Na_2CrO_4] is 350 g/L)

crystals grew to approximately 0.5 μm. An increasing number of thin plates were observed in the middle of the twinning crystals at 15 min after the M_p (Fig. 1). As time increased to 30 min, the morphology of the bayerite particles consisted mostly of microrods (1.0 μm) stacked neatly in piles of several thin plates (see Fig. 7(c)) as reported in the Ref. [29]. The polymorphs of bayerite consisted of layers of aluminum octahedra with hydroxyl groups. Hydrogen bonds connected the layers together. In the later stage, needle-shaped dawsonite and carbonates formed and twined around the bayerite (see Fig. 7(d)). However, the XRD pattern shows the presence of a small amount of dawsonite in the final sample. Some dawsonite phases may have been transformed into the bayerite phase in the carbonate solution during washing [25].

3.4.3 Impurity content

Precipitated $Al(OH)_3$ from supersaturated sodium aluminate solutions usually contains impurities such as sodium, iron, calcium and silicon. Sodium, usually calculated as Na_2O, is the major impurity in the alumina industry. Chromium (calculated as Cr_2O_3) is considered as another major impurity in bayerite precipitated from chromate alkali solutions.

As listed in Table 1, Cr_2O_3 and Na_2O contents in the bayerite were higher at low temperatures than those at high temperatures. The Na_2O content reached 2.19% at CO_2 volume fraction of 28.5% at 30 °C. These results show that gelatinous $Al(OH)_3$ with a high impurity content was precipitated from the chromate alkali solution. The impurity content decreased as the temperature increased from 30 to 50 °C, indicating that coarse particles absorbed less impurity on their surfaces.

Table 1 Impurity contents in bayerite obtained from chromate alkali solutions

Tempeatrue/	21.0% CO_2		28.5% CO_2	
°C	$w(Cr_2O_3)$/%	$w(Na_2O)$/%	$w(Cr_2O_3)$/%	$w(Na_2O)$/%
30	0.06	0.13	0.07	2.19
50	0.06	0.10	0.05	0.08
70	0.07	0.14	0.05	0.14
90	0.08	3.13	0.06	8.06

The Cr_2O_3 and Na_2O contents in the bayerite increased as the temperature increased from 50 to 90 °C under various CO_2 volume fractions. The Cr_2O_3 content was below 0.08% (mass fraction), whereas Na_2O significantly increased from 0.08% to 8.06%. These results indicate that both temperature and CO_2 volume fraction play important roles in increasing the impurity content in bayerite. The Cr_2O_3 content slightly increased because of the stable adsorption of chromate ions on the bayerite surface. The Na_2O content significantly increased as a result of $NaAlCO_3(OH)_2$ (dawsonite) formation, as described in Eq. (4). Bayerite with low impurity content was obtained under CO_2 volume fraction of 28.5% and at temperatures of 50−70 °C.

3.4.4 FT-IR spectroscopy

Figure 8 shows that the peaks at 3657 and 978 cm^{-1} correspond to bayerite [31]. Significant bands in the IR spectrum of bayerite include those at around 3657, 3550, 3473 and 3422 cm^{-1}, which correspond to OH stretching modes. No significant changes were observed in these bands.

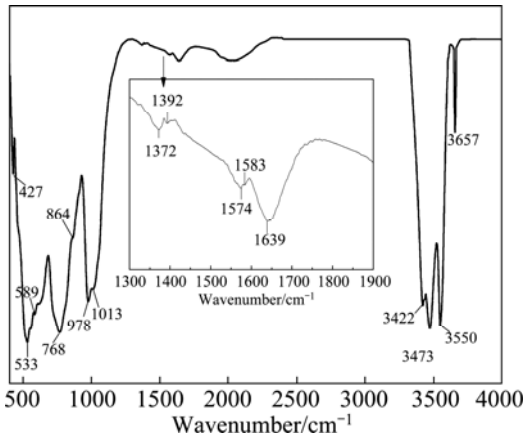

Fig. 8 FTIR spectra of bayerite (Temperature is 50 °C, [NaOH] is 33.35 g/L, CO_2 volume fraction is 28.5%, [Al_2O_3] is 10 g/L, [Na_2CrO_4] is 350 g/L)

The bands at 1027 and 982 cm^{-1}, which shift to 1012 and 978 cm^{-1}, are attributed to the OH bending bands of bayerite. The IR bands at 864, 768, 589, 533, and 427 cm^{-1} are also similar to those of bayerite. The 1639 cm^{-1} peak originates from free molecular water that is not coordinately bonded to an aluminum ion. The presence of absorbed molecular water was confirmed by peaks at 1392 and 1639 cm^{-1} as well as by the shoulder peak at around 1583 cm^{-1}. Meanwhile, the bands at 1372 and 1574 cm^{-1}, which are characteristic of chromia-alumina [32], may be attributed to chromates. These ions may have been absorbed on the bayerite surface during crystallization and appear on the layer edge or between the double layers of bayerite. However, the 885 cm^{-1} peak typical of CrO_4^{2-} was not observed. This peak may have overlapped by the high-intensity peaks of bayerite. Chromates and aluminum ions are held together by van der Waals forces. Therefore, a small amount of chromates absorbed on the bayerite may be difficult to wash away. To remove water-soluble chromates, some measures, including heating and salt treatment, must be taken to change the structure of the bayerite layers. The product can be used to make refractory materials, bricks and other products.

3.5 Mechanism of chromium and sodium incorporation into bayerite

During $Al(OH)_3$ precipitation from supersaturated sodium aluminate solutions, sodium aluminate ion pairs may be adsorbed at appropriate sites on the prismatic and basal faces and release sodium and hydroxyl ions to the solution during the restructuring to gibbsite [33]. Sodium ions may be incorporated between the double layers or substituted for protons because of their slow diffusion from the lattice of bayerite.

Bayerite structures adopt the $P_{21/n}$ space group, which consist of double layers stacked directly on top of each other, resulting in the ABABABAB... structure [34]. If the stacking varies, the X-ray lines of the certain planes are broadened, whereas other lines remain sharp. X-ray diffraction lines, such as (001) and (100), were found to be broadened by the stacking disorder (Table 2). The measured d spacing from (001) reached 4.73 Å at 50 °C and 4.74 Å at 70 °C, respectively. Sodium ions incorporated into the lattice may have been located near "active growth sites" on the surface layer and substituted for protons in the crystal lattice as a consequence of hydrogen bonding between the layers [33]. In addition, the incorporation also occurred on the edges of the layer.

The Cr_2O_3 content slightly varied under various conditions. Considering the adsorption of chromate in the layer structure of clay [35], chromate may have been adsorbed between the double layers of bayerite. Between 21.0% and 28.5% CO_2 at 70 °C, a slight difference was observed in the Cr_2O_3 content in bayerite but not in the Na_2O content (Table 1). The same diffraction line (001) was broadened (Table 2). Reflections from planes such as (100) and (111) remained sharp. Therefore, adsorption of chromate may also have occurred at "active growth sites", thereby affecting the adsorption of aluminate ions on the surface layer of bayerite. Secondary nucleation generally does not occur when growth sites are blocked. Although the supersaturation of the chromate alkali

Table 2 Calculated and measured d spacing under different conditions

Bayerite (00-012-0457)			50 °C, 28.5% CO_2		70 °C, 21.0% CO_2		70 °C, 28.5% CO_2	
2θ/(°)	(hkl)	d_{cal}/Å	$2\theta_{mea}$/(°)	d_{mea}/Å	$2\theta_{mea}$/(°)	d_{mea}/Å	$2\theta_{mea}$/(°)	d_{mea}/Å
18.79	(001)	4.72	18.76	4.73	18.74	4.73	18.72	4.74
20.35	(100)	4.36	20.31	4.37	20.29	4.38	20.26	4.38
27.95	(101)	3.19	27.83	3.21	27.81	3.21	27.79	3.21
40.80	(111)	2.21	40.60	2.22	40.59	2.22	40.57	2.22
53.55	(112)	1.71	53.19	1.72	53.18	1.72	53.17	1.72

solution remains, the probability of heterogeneous nucleation on the previous surface is reduced, and the restructuring of bayerite in the chromate alkali solution is slower than that in the pure sodium aluminate solution during either the nucleation step or the crystal growth step, as shown in Fig. 1.

During deposition, chromate ions trapped and subsequently incorporated into the lattice because these ions were unable to diffuse away from the interfacial layer. Although the chamfer face was developed during primary nucleation (Fig. 7(a)), chromate ions appeared to block adhesion on the basal faces, leading to the formation of plate-like crystals at the final stage (Fig. 7(d)). Chromate incorporation between the double layers was thought to disrupt the structure by forming weak bonds. The inclusion of foreign ions, such as sodium and chromate, may strengthen the bonding of the layers, thereby permitting the formation of larger bayerite crystals.

The results show that the Cr_2O_3 content is lower than the Na_2O content of all samples precipitated from the chromate alkali solution (Table 1). In addition, the Na_2O content in the bayerite from these samples is significantly lower than that in the gibbsite obtained from the previous work [33]. These results imply that incorporation of the two ions occurs simultaneously and at the same site on the surface layer of bayerite. A low Cr_2O_3 content can decrease the Na_2O content of the sample in the presence of a large amount of sodium chromate. However, the probability of incorporating chromate ions into the lattice is less than that of sodium ions, which may be due to the larger size of the chromate ion. Furthermore, the absorption of chromate ions leads to rapid saturation because the limit variation of the chromate content in bayerite is small. Differences between the two impurities are significantly affected by variations in layer stacking, hydrogen positions, energy stability and other factors [30].

4 Conclusions

1) $Al(OH)_3$ precipitation from chromate alkali solutions differs from that from pure sodium aluminate solutions under the same conditions. The neutralization curve was divided into three regions. The induction period of the alkali metal chromate solution was longer than that of pure aluminum solution, indicating low deposition rates of $Al(OH)_3$ as well as the formation of coarse bayerite particles.

2) Under the same conditions, the major phases of the final products obtained from pure sodium aluminate solution and chromate alkali solutions were dawsonite and bayerite, respectively. The results show that well-crystallized bayerite composed of agglomerates of rods and cone frustums may be obtained from chromate alkali solutions. The mean particle sizes of the bayerite were between 24.2 and 29.3 μm at CO_2 volume fraction of 28.5% and at temperatures of 50−70 °C. Low-impurity bayerite was obtained from the chromate alkali solution.

3) Sodium ions were incorporated between the double layers or substituted for protons because of their slow diffusion from the lattice. The adsorption of chromate may occur at the same active sites, thereby affecting the adsorption of aluminate ions on the surface layer of bayerite. Chromate ions appeared to block the adhesion of the next growth layer on the basal faces, leading to the formation of plate-like crystals. However, the probability of incorporating chromate ions into the lattice was less than that of sodium ions.

References

[1] LI Ping, XU Hong-bin, ZHANG Yi, LI Zuo-hu, ZHENG Shi-li, BAI Yu-lan. The effects of Al and Ba on the colour performance of chromic oxide green pigment [J]. Dyes and Pigments, 2009, 80(3): 287−291.

[2] SRIVASTAVA M, BALARAJU J N, RAVISHANKAR B, RAJAM K S. Improvement in the properties of nickel by nano-Cr_2O_3 incorporation [J]. Surface and Coatings Technology, 2010, 205(1): 66−75.

[3] SHEE D, SAYARI A. Light alkane dehydrogenation over mesoporous Cr_2O_3/Al_2O_3 catalysts [J]. Applied Catalysis A: General, 2010, 389(3−4): 155−156.

[4] NAKAYAMA O, IKENAGA N, MIYAKE T, YAGASAKI E, SUZUKI T. Production of synthesis gas from methane using lattice oxygen of NiO−Cr_2O_3−MgO complex oxide [J]. Industrial & Engineering Chemistry Research, 2010, 49(2): 526−534.

[5] ŞAHAN H, GÖKTEPE H, PATAT Ş, ÜLGEN A. Effect of the Cr_2O_3 coating on electrochemical properties of spinel $LiMn_2O_4$ as a cathode material for lithium battery applications [J]. Solid State Ionics, 2010, 181(31−32): 1437−1444.

[6] HOLTZ W J. Process for removal of alumina from aqueous alkali metal chromate solutions: US, 4173618 [P]. 1979−09−06.

[7] WANG Shao-na, ZHENG Shi-li, ZHANG Yi. Stability of $3CaO{\cdot}Al_2O_3{\cdot}6H_2O$ in $KOH+K_2CO_3+H_2O$ system for chromate production [J]. Hydrometallurgy, 2008, 90(2−4): 201−206.

[8] ZAHN, GMBH. Process for preparing alkali metal chromate solutions: GB, 1057678 [P]. 1963−10−02.

[9] FRICK D G, MORGAN T R, STREETER T L. Alumina removal from chromate leach liquors: US, 3899568 [P]. 1975−08−12.

[10] SMELLIE M A, BRANASTATTER G H. Production of chromium carbide and ferrochrome alloys: GB, 1532601A [P]. 1978−11−15.

[11] SPECKETER H, HENSCHEL G. Production of chromates with simultaneous recovery of alumina: US, 1760788 [P]. 1930−05−27.

[12] JOHNSTON M, CLARK M W, MCMAHON P, WARD N. Alkalinity conversion of bauxite refinery residues by neutralization [J]. Journal of Hazardous Materials, 2010, 182(1−3): 710−715.

[13] ÁLVAREZ-AYUSO E, NUGTEREN H W. Synthesis of dawsonite: A method to treat the etching waste streams of the aluminium anodizing industry [J]. Water Research, 2005, 39(10): 2096−2104.

[14] WANG Zhi, BI Shi-wen, YANG Yi-hong, YUAN Zhang-fu. Evolution of particle size and strength of hydrargillite from carbonization in seeded sodium aluminate liquors [J]. Journal of

Crystal Growth, 2005, 274(1−2): 218−225.
[15] LI Xiao-bin, QI Tian-gui, PENG Zhi-hong, LIU Gui-hua, ZHOU Qiu-sheng. Neutralization and separation of aluminum from caustic sodium chromate solution: CN, 101723461A [P]. 2010−06−09. (in Chinese)
[16] MISRA C. Solubility of aluminium trihydroxide in sodium hydroxide solution [J]. Chemical and Industry, 1970, 9: 619−623.
[17] SWEEGERS C, de CONINCK H C, MEEKES H, van ENCKEVORT W J P, HIRALAL I D K, RIJKEBOER A. Morphology, evolution and other characteristics of gibbsite crystals grown from pure and impure aqueous sodium aluminate solutions [J]. Journal of Crystal Growth, 2001, 233(3): 567−582.
[18] BROWN N. Effect of calcium ions on agglomeration of bayer aluminium trihydroxide [J]. Journal of Crystal Growth, 1988, 92(1−2): 26−32.
[19] MUHR H, LECLERC J P, PLASARI E, NOVELCATTIN F. A rapid method for the determination of growth rate kinetic constants: application to the precipitation of aluminum trihydroxide [J]. Industrial & Engineering Chemistry Research, 1997, 36(3): 675−681.
[20] PANIAS D, ASIMIDIS P, PASPALIARIS I. Solubility of boehmite in concentrated sodium hydroxide solutions: Model development and assessment [J]. Hydrometallurgy, 2001, 59(1): 15−29.
[21] LI Yan, ZHANG Yi-fei. YANG Chao, ZHANG Yi. Precipitating sandy aluminium hydroxide from sodium aluminate solution by the neutralization of sodium bicarbonate [J]. Hydrometallurgy, 2009, 98(1−2): 52−57.
[22] PANIAS D, KRESTOU A. Effect of synthesis parameters on precipitation of nanocrystalline boehmite from aluminate solutions [J]. Powder Technology, 2007, 175(3): 163−173.
[23] LI J, PRESTIDGE C A, ADDAI-MENSAH J. The influence of alkali metal ions on homogeneous nucleation of $Al(OH)_3$ crystals from supersaturated caustic aluminate solutions [J]. Journal of Colloid and Interface Science, 2000, 224(2): 317−324.
[24] LI Jie, CHEN Qi-yuan, YIN Zhou-lan. Studies on the kinetics of unneeded nucleation of aluminum trihydroxide from supersaturated sodium aluminate solutions [J]. Chemical Journal of Chinese Universities, 2003, 24(9): 1652−1656. (in Chinese)
[25] BÉNÉZETH P, PALMER D A, ANOVITZ L M, HORITA J. Dawsonite synthesis and reevaluation of its thermodynamic properties from solubility measurements: Implications for mineral trapping of CO_2 [J]. Geochimica et Cosmochimica Acta, 2007, 71(18): 4438−4455.
[26] HARRIS D R, KEIR R I, PRESTIDGE C A, THOMAS J C. A dynamic light scattering investigation of nucleation and growth in supersaturated alkaline sodium aluminate solutions (synthetic Bayer liquors) [J]. Colloids and Surfaces A: Physicochemical and Engineering Aspects, 1999, 154(3): 343−352.
[27] ADDAI-MENSAH J, RALSTON J. The influence of interfacial structuring on gibbsite interactions in synthetic bayer liquors [J]. Journal of Colloid and Interface Science, 1999, 215(1): 124−130.
[28] SAHU R C, PATEL R K, RAY B C. Neutralization of red mud using CO_2 sequestration cycle [J]. Journal of Hazardous Materials, 2010, 179(1−3): 28−34.
[29] LEFÈVRE G, FÉDOROFF M. Synthesis of bayerite (β-$Al(OH)_3$) microrods by neutralization of aluminate ions at constant pH [J]. Materials Letters, 2002, 56(6): 978−983.
[30] LEFÈVRE G, PICHOT V, FÉDOROFF M. Controlling particle morphology during growth of bayerite in aluminate solutions [J]. Chemistry of Materials, 2003, 15(13): 2584−2592.
[31] MUSIĆ S, DRAGČEVIĆ Đ, POPOVIĆ S, VDOVIĆ N. Chemical and microstructural properties of Al-oxide phases obtained from $AlCl_3$ solutions in alkaline medium [J]. Materials Chemistry and Physics, 1999, 59(1): 12−19.
[32] LITTLE L H, AMBERG C H. Infrared spectra of carbon monoxide and carbon dioxide adsorbed on chromia-alumina and on alumina [J]. Canadian Journal of Chemistry, 1962, 40: 1997−2006.
[33] WATLING H. Gibbsite crystallization inhibition: 2. Comparative effects of selected alditols and hydroxycarboxylic acids [J]. Hydrometallurgy, 2000, 55(3): 289−309.
[34] GALE J D, ROHL A L, MILMAN V, WARREN M C. An ab initio study of the structure and properties of aluminum hydroxide: Gibbsite and bayerite [J]. Journal of Physical Chemistry B, 2001, 105(42): 10236−10242.
[35] BHATTACHARYYA K G, SENGUPTA S. Adsorption of chromium (VI) from water by clays [J]. Industrial & Engineering Chemistry Research, 2006, 45(21): 7232−7240.

铬酸钠碱性液中拜耳石的结晶行为

魏广叶[1,2]，曲景奎[1]，郑裕东[2]，齐 涛[1]，郭 强[1]，韩冰冰[1]，赵宏欣[1]

1. 中国科学院 过程工程研究所，湿法冶金清洁生产技术国家工程实验室，北京 100190；
2. 北京科技大学 材料科学与工程学院，北京 100083

摘 要：铬酸钠碱性液中铝的脱除和铝化合物的利用是实现铬盐产品清洁生产的重要步骤。讨论铬酸钠对中和过程、氢氧化铝沉淀效率和氢氧化铝结晶诱导期的影响。结果表明：与高浓度铝酸钠相似，铬酸钠碱性液中铝酸钠的中和曲线也分为明显的 3 个区域。在相同铝浓度的溶液中，络酸钠碱性液中铝酸钠的诱导期比纯铝酸钠溶液的诱导期更长。温度和二氧化碳体积分数的降低有利于形成较为粗大的氢氧化铝颗粒。在温度为 50~70 °C，二氧化碳浓度为 28.5%(体积分数)时，氢氧化铝主要为拜耳铝石型，由棒状和圆台状的聚集体组成。颗粒尺寸(d_{50})在 24.2 μm 到 29.3 μm 之间，杂质较少，有利于产品的综合利用。

关键词：铬酸钠碱性液；拜耳铝石；碳分；结晶；沉积效率

(Edited by Chao WANG)